Impact of Reynolds and Prandtl Numbers Coupled with Viscous Dissipation on Mixed Convection in A Square Cavity

EMMANUEL O. SANGOTAYO[1,*], NIKOS MASTORAKIS[2]
[1]Department of Mechanical Engineering,
Ladoke Akintola University of Technology, Ogbomoso,
NIGERIA

[2]Technical University of Sofia,
Sofia,
BULGARIA

**Corresponding Author*

Abstract: - Efficient thermal management in industrial manufacturing and electronic cooling systems can be achieved by comprehending characteristics of Reynolds and Prandtl numbers in mixed convection scenarios, which aids in the optimization of heat transfer systems through the utilization of forced and natural convection effects. The impact of Reynolds and Prandtl numbers on mixed convection in a square cavity connected to a moving heated horizontal plate is investigated in this research paper. The convective behavior under different conditions was evaluated by discretizing the flow governing equations, which included the momentum and energy equations, using the finite difference method. The research assessed various fluids, including air (Pr = 0.7), liquid metal (Pr = 0.01), and oil (Pr = 10). The Reynolds number ranged from 0.001 to 100, the Eckert number ranged from 0.01 to 40, and a constant Richardson number (Ri = 1) was maintained throughout. The results revealed that the Reynolds number substantially impacts the velocity and temperature characteristics, especially when coupled with a Prandtl number over one and when viscous dissipation remains constant. The utmost velocity that can be attained within the cavity is significantly diminished as the Reynolds number rises, underscoring the critical importance of dynamic fluid properties in determining heat transfer efficiency and fluid flow characteristics. The research unveiled the critical importance of Reynolds and Prandtl numbers in the field of fluid dynamics concerning enhancing heat transfer attributes for engineering purposes, thereby guaranteeing the effectiveness of thermal systems.

Key-Words: - Reynolds number, Prandtl number, moving plate, finite difference method, heat transfer, fluid dynamics.

Received: January 16, 2024. Revised: August 11, 2024. Accepted: September 7, 2024. Published: October 21, 2024.

1 Introduction

The study of mixed convection flow and heat transfer in lid-driven enclosures has received significant interest in academic literature. Conjugate mixed convection heat transfer is applied in a wide range of engineering and natural processes. These include cooling electronic components, lubrication technologies, drying processes, food production, flow and heat transfer in solar ponds, and the thermal-hydraulics of nuclear reactors. Flow and heat transfer occur frequently in obstructed enclosures in various technical applications, such as improving heat transfer efficiency in microelectronic devices, flat-plate solar collectors, and flat-plate condensers in refrigeration systems. These specific matters have primarily been investigated about natural convection occurring within enclosed spaces. [1], performed a study on the properties of natural convective flow and heat transfer around a heated cylinder placed inside a square area with different thermal boundary conditions. In addition, [2], conducted a detailed investigation of the combined effects of natural convection and conduction within a complex enclosure. The findings revealed a clear correlation between thermal conductivity in the solid region and the improvement of flow and heat transfer. The total flow and heat transfer dynamics were shown to be considerably affected by geometric forms and Rayleigh numbers.

[3], conducted a study on the natural convection processes occurring in a closed cavity

of a refrigerator. Similarly, [4], used numerical techniques to investigate the continuous flow of heat caused by natural convection in a square container filled with a fixed amount of solid material that conducts heat that contains circular or square barriers. The investigation showed a minor variation in the average Nusselt number between cylindrical rods and square rods. [5], conducted a separate investigation on natural convection in a horizontal fluid layer that contained a conducting body. They utilized a precise and efficient Chebyshev spectral collocation approach and [6] furthered their research by examining spontaneous convection in a horizontal fluid layer that contained a heat-generating conducting body. In addition, [7], examined the phenomenon of natural convection around a heated square cylinder that was positioned inside an enclosure, with the Rayleigh number varying between 10^3 and 10^6. The work focused on analyzing the intricate flow and heat transfer properties under different thermal boundary circumstances, revealing precise differences between heating with uniform wall temperature and heating with uniform wall heat flux. The use of enclosures with movable lids is of utmost significance in the field of heat transfer mechanisms, especially in applications such as cooling electronic chips, harnessing solar energy, and the food industry. [8], investigated the impact of the Prandtl number on both the flow patterns and the mechanisms of heat transmission in a square container. The results revealed that the influence of buoyancy becomes more noticeable as the Prandtl number increases. Additionally, the authors derived a correlation between the average Nusselt number and the Prandtl number, Reynolds number, and Richardson number. A numerical analysis of heat transport through mixed convection in a two-dimensional square cavity with an aspect ratio of 1 was conducted by [9].

2 Physical Domain

The flow of mixed convection around a heated bluff body with a square cross-section is a fundamental engineering problem that is relevant in several practical scenarios. These scenarios include heat exchangers, chemical industries, electronic cooling, and the flow around buildings, among others. The flow around unheated square barriers is characterized by the interplay of a free shear layer, a boundary layer that forms on the surfaces of the obstacle. Heating a cylinder causes the added buoyancy to greatly complicate the flow. The quantification of the buoyancy effect is done using a non-dimensional metric called the Richardson number. This number indicates the ratio of the buoyancy force to the inertial force. The flow field surrounding a hot object is mainly influenced by the Reynolds number (Re), Richardson number (Ri), and Prandtl number (Pr).

Several empirical and computational investigations have been carried out to analyze the influence of these parameters on fluid dynamics. The impact of Reynolds number (Re) on the flow over a square cylinder has been recorded by several studies, [10], [11]. When a cylinder is placed in a free stream, the flow remains constant for Reynolds numbers (Re) below 40 and becomes irregular for Re values beyond 50, [12]. At low Reynolds (Re) values, there is no separation of flow at the leading and trailing edges of the cylinder, resulting in the top and bottom surfaces behaving similarly to a flat plate. As a result, the transfer of heat is highest at the surfaces close to the front corners and decreases towards the rear corners, [13]. Many scholars have extensively studied the influence of buoyancy on the flow field surrounding a square cylinder and vortex shedding occurs in a cross-buoyancy flow scenario for all Ri values in the unstable flow regime, as shown by [14]. However, in the steady flow regime, [15] found that vortex shedding begins after a threshold Ri value. The reduction of vortex shedding is observed after attaining a threshold Ri value, which helps to enhance buoyancy, [16]

According to [17], the requirement for a certain Re value to initiate flow separation becomes more important as the Ri value increases. The increase in Ri was associated with a greater length of vortex formation, resulting in the suppression of vortex shedding, [18]. The Prandtl number (Pr) is a crucial factor that affects the flow field. It is calculated by dividing the momentum diffusivity by the thermal diffusivity in the fluid. The range of values varies significantly, ranging from approximately 0.001 for liquid metals to 1025 for the Earth's mantle. Fluids with varying Prandtl numbers are widely used in chemical industries and nuclear reactors. However, there have been few studies that have examined the influence of Pr on the flow around a square cylinder.

[19], investigated the impact of Prandtl number (Pr) on the restricted cross buoyancy flow around a square cylinder positioned in a channel under constant flow circumstances, with Pr values ranging from 0.7 to 100. The behavior of streamlines, isotherms, and drag and lift coefficients for different Pr values was demonstrated. [20], examined the impact of

the Prandtl number (Pr) on the phenomenon of unstable forced convection around a square cylinder. It was found that the Nusselt number, which represents the convective heat transfer over the surface of the cylinder, rose as the Prandtl number grew. [21], examined the movement of fluid around two square cylinders placed one after the other, with a constant and controlled flow, for a range of Prandtl numbers from 0.7 to 1000. It was observed that when the Pr values were low, the isotherms were wider, and when the Pr values were high, the isotherms became narrower as a result of decreased thermal diffusion. [22], investigated the movement of fluid with different densities passing between two square cylinders arranged in a line. They conducted their study for a range of Prandtl numbers (Pr) between 0.7 and 100, while maintaining a constant flow rate. As the Pr values increased, they saw a decrease in the asymmetry caused by buoyancy in the flow field. Additionally, at higher Pr values, there was a less pronounced change in the lift coefficient with Ri. The current investigation examined the flow of a heated rectangular cavity under specific conditions: 0.001 < Prandtl number (Pr) < 10, 0.001 < Reynolds number (Re) = 100, 0.01 < Eckert number (Ec) = 40, with a Richardson number (Ri) of 1. This study investigated the impact of changing the Reynold number and Prandtl number, along with the viscous-energy dissipation function, on the flow patterns, energy distribution, and heat transfer rate within a rectangular cavity.

2.1 The Physical and the Mathematical Models

Figure 1 illustrates the continuous motion of a horizontal plate emerging from a slot at a velocity Uw and temperature Tw into a quiescent fluid within a rectangular enclosure. This plate serves as the upper boundary of the enclosure, which is also defined by a fixed horizontal isothermal wall at the bottom, a fixed isothermal vertical wall on the left, and an adiabatic vertical wall on the right. The upper horizontal wall's temperature Tw is higher than the lower horizontal wall (i.e. Tw > T∞), leading to free convective motion within the enclosure. The flow is considered steady, incompressible, laminar, and two-dimensional, with the fluid being Newtonian. Negligible heat transfer by radiation and internal heat generation is assumed while accounting for the viscous-energy dissipation function effect. The fluid properties are assumed to be temperature-independent except for the buoyancy term in the momentum equation, for which the Boussinesq approximation is utilized. The extrusion die wall is both stationary and impermeable, imposing non-slip boundary conditions.

The governing equations for the flow at each point in the continuum consist of mass, momentum, and energy conservation expressions, including the viscous dissipation term, these equations for a two-dimensional rectangular domain are as presented in equations (1-6):

Continuity equation:

$$\frac{\partial u}{\partial x}+\frac{\partial v}{\partial y}=0 \tag{1}$$

The Navier-Stokes equations in the x- and y-directions as presented in equations (2 and 3):

$$u\frac{\partial u}{\partial x}+v\frac{\partial u}{\partial y}=-\frac{1}{\rho}\frac{\partial p}{\partial x}+\nu\left(\frac{\partial^2 u}{\partial x^2}+\frac{\partial^2 u}{\partial y^2}\right) \tag{2}$$

$$u\frac{\partial v}{\partial x}+v\frac{\partial v}{\partial y}=u\frac{\partial v}{\partial x}+v\frac{\partial v}{\partial y}= -\frac{1}{\rho}\frac{\partial p}{\partial y}+\nu\left(\frac{\partial^2 v}{\partial x^2}+\frac{\partial^2 v}{\partial y^2}\right)+\beta g\left(T-T_\infty\right) \tag{3}$$

where $\beta g\left(T-T_\infty\right)$ is the body force per unit volume in the y-direction.

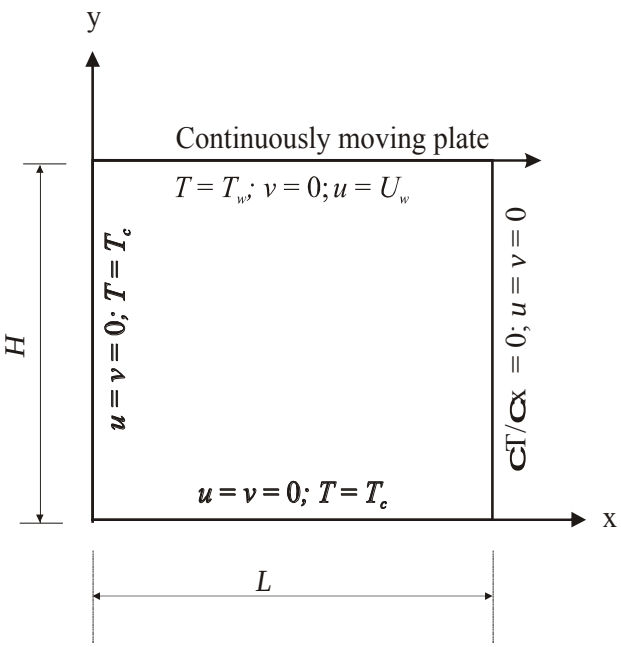

Fig. 1: Schematic representation of the physical model with the boundary constraints and the coordinate axes

The thermal energy transport equation is expressed in equation (4):

$$\rho c_p\left(u\frac{\partial T}{\partial x}+v\frac{\partial T}{\partial y}\right)= k\left(\frac{\partial^2 T}{\partial x^2}+\frac{\partial^2 T}{\partial y^2}\right)+\mu\phi \quad (4)$$

where ϕ represents the viscous-energy-dissipation function, defined by equation (5):

$$\phi = 2\left(\left(\frac{\partial u}{\partial x}\right)^2+\left(\frac{\partial v}{\partial y}\right)^2\right)+\left(\frac{\partial v}{\partial x}+\frac{\partial u}{\partial y}\right)^2 \quad (5)$$

The consideration of this function becomes crucial in cases of high fluid viscosity or flow velocities.

The specified boundary conditions for velocities and temperature are:

$$u=U_w,\ v=0,\ T=T_w \text{ at } y=H,\ 0\le x\le L;$$
$$u=0,\ v=0,\ T=T_\infty \text{ at } y=0,\ 0\le x\le L;$$
$$u=0,\ v=0,\ T=0 \text{ at } x=0,\ 0\le y\le H;$$
$$\frac{\partial u}{\partial x}=\frac{\partial v}{\partial x}=\frac{\partial T}{\partial x}=0 \text{ at } x=L,\ 0\le y\le H. \quad (6)$$

3 Procedure of Analysis and the Solution Techniques

The Navier-Stokes equations represent a group of partial differential equations that can be categorized as elliptic, parabolic, or hyperbolic based on the specific problem being addressed. When considering these equations in their incompressible form, one can opt to solve them using either the vorticity-stream function approach or in their primitive-variable form. For this study, the former method is employed resulting in equations (2) and (3) being simplified into a vorticity transport equation by removing the pressure gradient terms through the use of the continuity equation (1), along with the scalar value of the vorticity, w, in a two-dimensional Cartesian coordinate system defined in equation (7):

$$\omega=\frac{\partial v}{\partial x}-\frac{\partial u}{\partial y}. \quad (7)$$

This derived expression manifests as the dimensional vorticity transport equation (8):

$$u\frac{\partial \omega}{\partial x}+v\frac{\partial \omega}{\partial y}=-\beta g\frac{\partial T}{\partial x}+\upsilon\left(\frac{\partial^2 \omega}{\partial x^2}+\frac{\partial^2 \omega}{\partial y^2}\right) \quad (8)$$

The velocity components within a two-dimensional Cartesian coordinate system are delineated as derivatives of the stream function, as indicated in eqn(9):

$$u=\frac{\partial \psi}{\partial y},\quad v=-\frac{\partial \psi}{\partial x} \quad (9)$$

Upon substitution into equation (7), the Poisson equation for the stream function is obtained in eqn (10):

$$\omega=-\left(\frac{\partial^2 \psi}{\partial x^2}+\frac{\partial^2 \psi}{\partial y^2}\right) \quad (10)$$

The energy equations developed alongside the prescribed boundary conditions were transformed into non-dimensional form to allow for generalization across various physical scenarios using L, $(T_w - T_\infty)$, U_W, $U_W L$ and U_W/L respectively for length, temperature, velocity, stream function, and vorticity as presented in equation (11) :

$$X=\frac{x}{L},\quad Y=\frac{y}{L},$$
$$U=\frac{u}{U_w},\quad V=\frac{v}{U_w},$$
$$\theta=\frac{(T-T_\infty)}{(T_w-T_\infty)},\quad \Psi=\frac{\psi}{U_w L},$$
$$\Omega=\frac{\omega}{U_w/L}, \quad (11)$$

The normalized versions of the X- and Y-velocity components, stream function, vorticity, and energy transport equations are presented in equations (12-15):

$$U=\frac{\partial \psi}{\partial Y},\quad V=-\frac{\partial \psi}{\partial X} \quad (12)$$

$$-\Omega=\frac{\partial^2 \Psi}{\partial X^2}+\frac{\partial^2 \Psi}{\partial Y^2} \quad (13)$$

$$U\frac{\partial\Omega}{\partial X}+V\frac{\partial\Omega}{\partial Y}= \frac{1}{Re}\left(\frac{\partial^2\Omega}{\partial X^2}+\frac{\partial^2\Omega}{\partial Y^2}\right)-\frac{Gr}{Re^2}\frac{\partial\theta}{\partial X} \quad (14)$$

$$U\frac{\partial\theta}{\partial X}+V\frac{\partial\theta}{\partial Y}=\frac{k}{\mu C_p Re}\left(\frac{\partial^2\theta}{\partial X^2}+\frac{\partial^2\theta}{\partial Y^2}\right)+ \left(\frac{Ec}{Re}\right)\left[2\left(\left(\frac{\partial U}{\partial X}\right)^2+\left(\frac{\partial V}{\partial Y}\right)^2\right)+\left(\frac{\partial V}{\partial X}+\frac{\partial U}{\partial Y}\right)^2\right] \quad (15)$$

Within the equations (14-15), Ec represents the Eckert number, k denotes thermal conductivity, μ signifies dynamic viscosity, Cp stands for specific heat capacity, Re represents the Reynolds number, and Gr represents the Grashof number. The Eckert number serves to relate the flow viscous-dissipation term to energy distributions. This number acts as a criterion for determining the inclusion of the viscous-energy dissipation effect in heat transfer analysis. The Prandtl number establishes a link between the rates of heat and momentum diffusion. The Grashof number serves as a dimensionless parameter reflecting the ratio of buoyancy force to viscous force in free-convection flow issues, it signifies whether the flow is laminar or turbulent, and which dynamic process holds dominance.

The boundary conditions, when expressed in non-dimensional form, are as follows:

$$\Omega\neq 0;\ \Psi\neq 0;\ \mathrm{V}=0;\ \mathrm{U}=\theta=1 \quad \text{at } \mathrm{Y}=1;\ 0\le \mathrm{X}\le 1\ ;$$

$$\Omega\neq 0\ ;\ \Psi=U=V=\theta=0 \quad at\ Y=0;\ 0\le X\le 1\ ;$$

$$\Omega\neq 0\ ;\ \Psi=U=V=\theta=0 \quad at\ X=0;\ 0\le Y\le 1\ ;$$

$$\Omega\neq 0;\ \Psi=\frac{\partial \mathrm{U}}{\partial \mathrm{X}}=\frac{\partial \mathrm{V}}{\partial \mathrm{X}}=\frac{\partial\theta}{\partial \mathrm{X}}=0 \quad \text{at } \mathrm{X}=1;\ 0\le \mathrm{Y}\le 1 \quad . \quad (16)$$

The vorticity and energy transport equations (14) and (15) exhibit non-linear characteristics. Currently, there are no universally accepted analytical solutions available for these interconnected equations. Among the most effective methods for solving equations (12) – (15) is the finite difference technique, where each term within the differential equations is approximated by their corresponding differential quotient. The resulting linear equations are subsequently addressed concurrently by employing the relaxation technique.

The convective heat transfer inside the enclosure is calculated based on the Nusselt number, a dimensionless quantity that characterizes the proportion of heat transfer via convection and conduction across the fluid layer. The temperature gradient resulting from the exchange of heat between the fluid and the wall can be associated with the local Nusselt number, Nu_x, through Equation (17):

$$Nu_x=\frac{h_x x}{k}=-\left(\frac{\partial\theta}{\partial Y}\right)_{Y=1} \quad (17)$$

The mean Nusselt number is derived through the integration of the local Nusselt number along the entire length of the heated wall as shown in Equation (18):

$$N\bar{u}=\frac{\dot{Q}_{conv}}{\dot{Q}_{cond}}=-\int_0^1\left.\frac{\partial\theta}{\partial Y}\right|_{Y=0\ or\ 1}dX \quad (18)$$

The attainment of a stable flow state was determined by monitoring the convergence of temperature and vortex field, utilizing the prescribed criterion given by Equation (19):

$$\frac{\sum_{i=2}^{N}\sum_{j=2}^{M}\left|\phi_{ij}^{n+1}-\phi_{ij}^{n}\right|}{\sum_{i=2}^{N}\sum_{j=2}^{M}\left|\phi_{ij}^{n+1}\right|}<\delta \quad (19)$$

The parameter δ represents α, θ, or ω, with n indicating the number of iterations until the results converge. The literature reports variations in the value of δ ranging from 10^{-3} to 10^{-8}, [23].

4 Discussion of Numerically Generated Results

An investigation was conducted to assess the influence of the convergence criterion on the numerical results. This was accomplished by calculating the mean Nusselt number for various values of the convergence parameter, δ which ranged from 10^{-1} to 10^{-8}. The results, shown in Figure 2, indicate that a δ value of 10^{-4} was enough

to achieve convergence. To verify the code used in this study and the precision of the simulations, the Nusselt number was calculated for a convective flow situation with a Prandtl number of 0.7 and a Rayleigh number of 1000. The Nusselt number calculated using the program was Nu = 1.1210, which closely matches the value of Nu = 1.132 given by [24] for the same Prandtl and Rayleigh values, with a discrepancy of around 2%. Additional validation was conducted by calculating the Nusselt number for a Rayleigh number (Ra) of 10^5 and a Prandtl number (Pr) of 0.7., [24], documented 4.6201, and the current simulation produced Nu = 4.7438, indicating consistent findings across the three investigations.

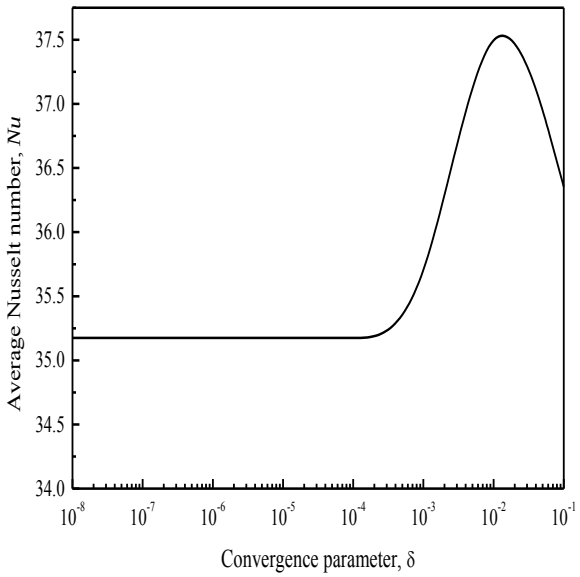

Fig. 2: Plot of average Nusselt number, *Nu* versus the convergence parameter, δ

The numerical results were rigorously validated to ensure grid independence. This was done by obtaining solutions using progressively larger grid sizes until a point was reached where a significant change in the solutions occurred with further increases in the number of nodes. This is shown in Figure 3 for Re = 100, Pr = 0.7, and Ra = 1000, represented by a dotted line. The accuracy of the computed numerical results was found to be highly dependent on the number of nodal points. The numerical results closely matched several well-established benchmarks using a grid structure consisting of 41 × 41 nodal points. The grid independence tests demonstrated that a grid system with dimensions of 41 × 41 was sufficient in terms of numerical stability, field resolution, and accuracy, which aligns with the conclusions of a previous study conducted by [23], [25].

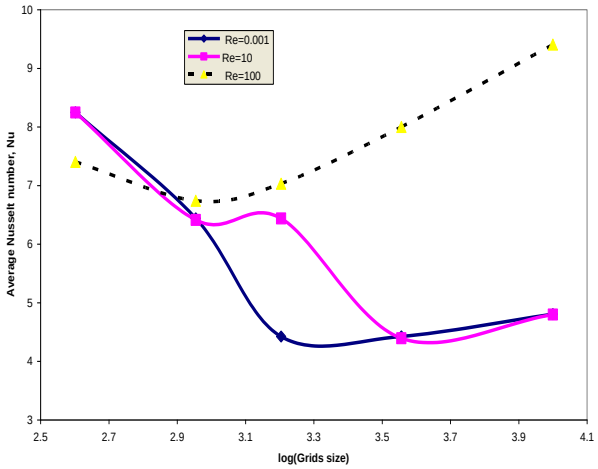

Fig. 3: Average Nusselt number, Nu versus log (Grid sizes) with different Reynolds numbers, Re, for Pr=0.7, Ra=1000

Figure 4 shows the non-dimensional temperature distribution at Y = 0.5 for various Eckert numbers (Ec), with Ra = 1000, Pr = 0.7, and Re = 100. The data illustrates that an elevation in the Eckert number results in an intensified temperature gradient. The Eckert number quantifies the relationship between the dynamic temperature resulting from fluid motion and the optimum temperature gradient of the fluid flow. The study concludes that the Eckert number has a considerable impact on the temperature gradient, especially at higher altitudes where there are matching strong temperature gradients. This discovery supports the research conducted by [23], which emphasizes the significant influence of viscous energy dissipation in flows with high-temperature gradients.

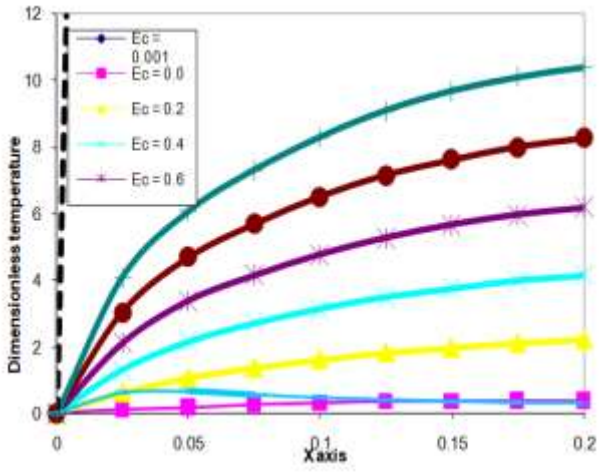

Fig. 4: Temperature distributions at Y = 0.5, with varying Eckert numbers, for given values of Ra = 1000, Pr = 0.7, and Re = 100

Figure 5 displays temperature profiles that have been scaled to remove units of measurement for different Prandtl numbers, Pr, at a specific location Y = 0.5. The values of Ra, Re, and Ec are fixed at 1000, 100, and 0.4, respectively. The diagram illustrates the impact of the Prandtl number on thermal patterns. The relationship between greater Prandtl numbers and enhanced temperature gradients in various fluids is apparent; it was supported by [8]. On the other hand, when the Prandtl number (Pr) is less than 1, there are only small variations in temperature gradient. This is due to either weak convection (low momentum diffusivity) or strong thermal diffusivity. This figure highlights the influence of the Prandtl number on temperature profiles, demonstrating a significant reduction in the thickness of the thermal boundary layer as the surface temperature differential increases.

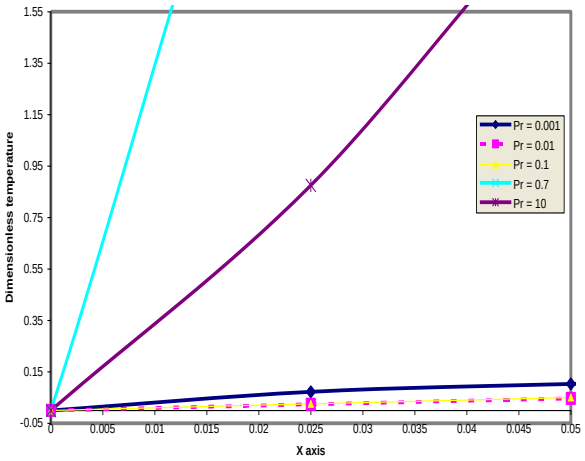

Figure 4.7 Temperature fields with different Prandtl numbers, Pr, at Y = 0.5, for Ra = 1000, Re = 100, Ec = 0.4

Fig. 5: Temperature distributions with varying Prandtl numbers, at Y = 0.5, for given values of Ra = 1000, Ec = 0.4, and Re = 100

Figure 6 depicts the dimensionless temperature distribution for various Reynolds numbers, labeled as Re, at a specific location Y = 0.5. The parameters Pr = 0.7, Ec = 0.4, and Ra = 1000 are also considered. The results suggest that as the Reynolds number increases, there is a proportional increase in the thermal fields, as evidenced by the temperature gradient. The figure demonstrates that when the Reynolds number (Re) is much smaller than 1, the thermal fields exhibit minor alterations. Nevertheless, when the Reynolds (Re) values reach 50, 70, 80, 90, and 100, the fields experience a sudden rise and converge at a shared point positioned at x = 0.4. Beyond this point, any further alterations in the fields become negligible. This pattern is caused by the prevalence of inertia forces over viscous forces in the fluid flow.

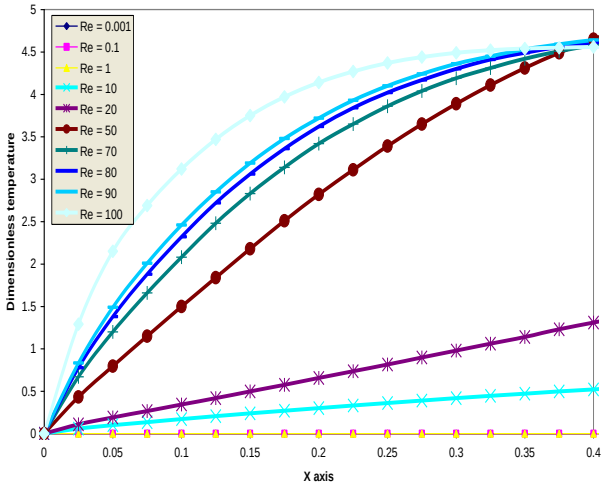

Figure 4.8 Temperature fields with different Reynolds numbers, Re, at Y = 0.5, for Pr = 1000, Ec = 0.4, Pr = 0.7

Fig. 6: Dimensionless temperature distribution for various Reynolds numbers, Re, at Y = 0.5 for Pr = 0.7, Ec = 0.4, and Ra = 1000

Figure 7 depicts the non-dimensional maximum stream function profile for different Eckert numbers while keeping the values of Ra = 1000, Pr = 0.7, and Re = 100 constant. The illustrated diagram demonstrates that the Eckert number has a negligible impact on the flow fields. More precisely, an increase in the Eckert number does not cause major changes in the flow patterns.

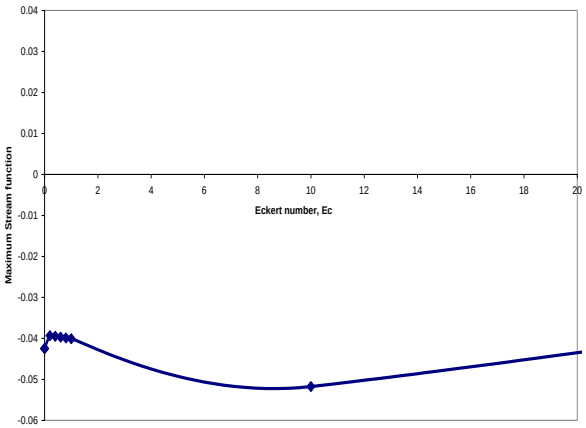

Figure 4.9 Effect of Eckert number on convective flow regimes as related by the maximum stream function, for Re = 100, Ra = 1000 and Pr = 0.7

Fig. 7: Dimensionless maximum stream function profile for different Eckert numbers, at Ra = 1000, Pr = 0.7, and Re = 100

Figure 8 displays non-dimensional streamline profiles corresponding to different Prandtl numbers, Pr, while keeping the circumstances fixed at Ra = 1000, Re = 100, and Ec = 0.4. The figure's representation demonstrates that an increase in the Prandtl number results in a decrease in the flow fields. Convection has a significantly reduced impact on the fields in the case of liquid metal. The Prandtl number is a measure of the material characteristics of a fluid, which might vary among

various fluids. A Prandtl number below 1 indicates either low momentum diffusivity (indicating weak convection) or high thermal diffusivity. This number is used to quantify the correlation between the rates at which heat and momentum diffuse, which is crucial in calculating the thickness of boundary layers in a specific external flow field. Increased momentum or thermal diffusivity indicates that the effects of viscosity or temperature spread over a larger area inside the flow field.

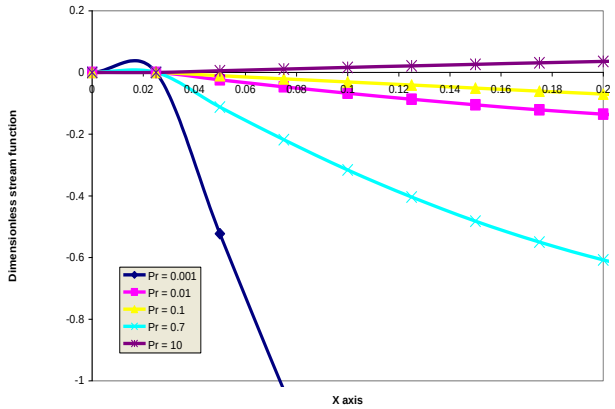

Figure 4.13 Flow fields with different Prandtl numbers, Pr. at Y = 0.5, for Ra = 1000, Re = 100, Ec = 0.4.

Fig. 8: Dimensionless streamline profiles corresponding to different Prandtl numbers, Pr, at mid-plane, for Ra = 1000, Re = 100, and Ec = 0.4

Figure 9 displays the non-dimensional streamline profile for different Reynolds numbers, Re while keeping Ra = 1000, Pr = 0.7, and Ec = 0.4 constant. The findings indicate that as the Reynolds number rises, there is a corresponding increase in the flow fields. This discovery emphasizes the dominant impact of inertia force compared to viscous force. When the Reynolds number (Re) is much less than 1, the flow fields experience little changes because the dominant force in the fluid flow is viscosity, rather than inertia. In this situation, diffusion is less significant compared to the inertial and buoyant forces within the enclosure.

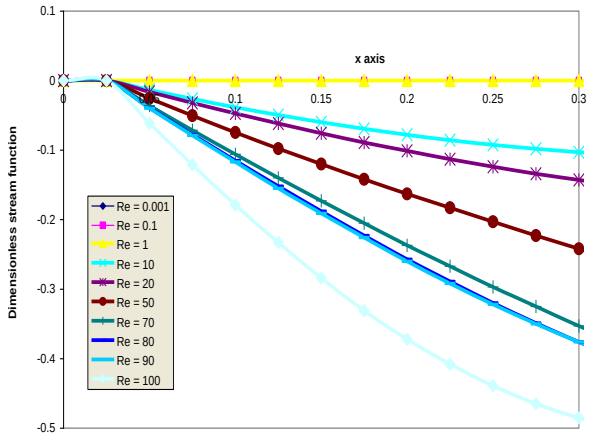

Figure 4.14 Flow fields with different Reynolds numbers, Re, at Y = 0.5, for Ra = 1000, Ec = 0.4, Pr = 0.7

Fig. 9: Dimensionless streamlines profile for different Reynolds numbers, Re, for Ra = 1000, Pr = 0.7, and Ec = 0.4

Figure 10 illustrates the relationship between the Nusselt number (Nu) and the Prandtl number (Pr) for different values of the Eckert number (Ec). The graph shows the Nu-Pr relationship for Ra = 1000, Ec = 0.4, and 0.0, with Re fixed at 100. The findings demonstrate that a higher Prandtl number corresponds to an increase in the Nusselt number.

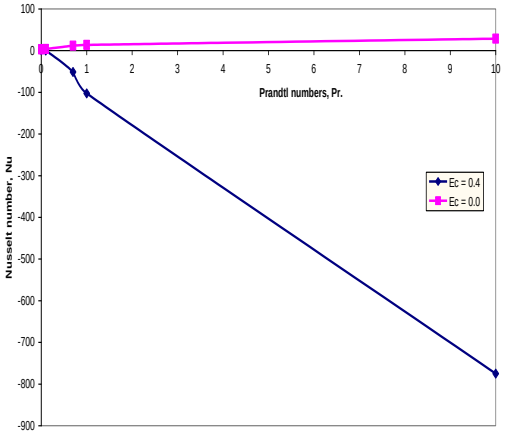

Figure 4.15 Nuselt number, Nu versus Prandtl numbers, Pr. for Ra = 1000, Re = 100,

Fig. 10: plot of Nu against Pr for Ra = 1000, Ec = 0.4, and 0.0, with Re fixed at 100.

Figure 11 depicts the graph of the Nusselt number, Nu, against the Reynolds number, Re, for Eckert numbers, Ec = 0.4, Ra = 1000, and Pr = 0.7. The obtained data demonstrates that when the Reynolds number increases, the Nusselt number displays harmonic patterns that are associated with energy-viscous-dissipation. The graphical representation suggests that the Reynolds number has a notable influence on the heat transfer properties within this particular region. Furthermore, at lower Reynolds numbers, the influence on the rate of heat transfer by different convection modes is insignificant because the diffusion effects decrease in both the inertial and buoyancy forces near the extrusion slot.

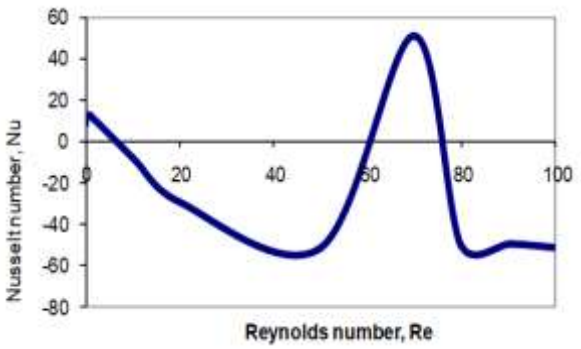

Fig. 11: Nusselt number, Nu versus Reynolds number, Re, for Pr = 0.7, Ra = 1000, Ec = 0.4

5 Conclusions

The study examined the heat transfer characteristics, flow patterns, and thermal distributions on a constantly moving horizontal sheet of extruded material in a stable fluid environment. This analysis was conducted both near and far from the extrusion slot and the numerical model was discretized using a central finite difference method. The study investigated the influence of the Prandtl number and Reynolds numbers at various values of the Eckert number on the thermal distributions, flow patterns, and heat transfer rates. The following findings were derived based on the analyzed flow conditions and parameter ranges:

The Eckert number has a substantial effect on the distribution of energy and the transfer of heat. It improves the distribution of energy without having a noticeable impact on the patterns of flow. An increase in Prandtl numbers results in enhanced thermal distributions and heat transfer rates, although it leads to diminished flow patterns. At lower Reynolds numbers, the heat transfer rates from distinct convection modes show negligible changes. However, as the Reynolds numbers increase, the thermal distributions, flow patterns, and heat transfer rates become more pronounced.

The findings of this research underscore the considerable significance of fluid dynamics in optimizing heat transfer for the benefit of engineering. Additional research that expand the range of Reynolds and Prandtl numbers so that the effects in various industrial and technological settings were thoroughly elucidated and ultimately contributed to the enhancement of thermal system design and performance.

Declaration of Generative AI and AI-assisted Technologies in the Writing Process

During the preparation of this work the authors used Grammarly for language editing. After using this service, the authors reviewed and edited the content as needed and take full responsibility for the content of the publication

References:

[1] Roychowdhury, D.G, Das, S.K., Sundararajan, T.S., (2002). Numerical simulation of natural convection heat transfer and fluid flow around a heated cylinder inside an enclosure, *Heat and Mass Transfer*, 38, 565-576.

[2] Dong, S. F., Li, Y.T., (2004). The conjugate of natural convection and conduction in a complicated enclosure, *Int. J. of Heat and Mass Transfer*, 47, 2233-2239.

[3] Hasanuzzaman, M., Saidur, R. and Masjuki, H. H., (2009). Effects of operating variables on heat transfer, energy losses and energy consumption of household refrigerator-freezer during the closed door operation, *Energy*, 34(2), 196-198.

[4] Braga, E. J., de Lemos, M. J. S., (2005). Laminar natural convection in cavities filed with circular and square rods, *Int. Commun. in Heat and Mass Transfer*, 32, 1289-1297.

[5] Lee, J. R., Ha, M. Y., (2005). A numerical study of natural convection in a horizontal enclosure with a conducting body, *Int. J. of Heat and Mass Transfer*, 48, 3308-3318.

[6] Lee, J. R., Ha, M. Y., 2006. Numerical simulation of natural convection in a horizontal enclosure with a heat-generating conducting body, *Int. J. of Heat and Mass Transfer*, 49, 2684-2702.

[7] Kumar D, A., Dalal, A., (2006). A numerical study of natural convection around a square, horizontal, heated cylinder placed in an enclosure, *Int. J. of Heat and Mass Transfer*, 49, 4608-4623.

[8] Moallemi, M. K., Jang, K. S., (1992). Prandtl number effects on laminar mixed convection heat transfer in a lid-driven cavity, *Int. J. Heat and Mass Transfer*, 35, 1881- 1892.

[9] Aydin, O., Yang, W. J., (2000). Mixed convection in cavities with a locally heated lower wall and moving sidewalls, *Numer. Heat Transfer*, Part A, 37, 695-710.

[10] Franke, R., Rodi W. and Schönung B. (1990). Numerical calculation of laminar vortex shedding flow past cylinders. *Journal of Wind Engineering and Industrial Aerodynamics,* 35, 237-257.

[11] Robichaux, J., S. Balachandar and S. P. Vanka (1999). Three-dimensional Floquet instability of the wake of a square cylinder. *Physics of Fluids*, 11, 560-578.

[12] Sharma, A. and Eswaran V. (2004a) Heat and fluid flow across a square cylinder in the two-dimensional laminar flow regime. *Numerical Heat Transfer, Part A: Applications*, 45, 247- 269.

[13] Rahnama, M. and Hadi-Moghaddam H. (2005). Numerical investigation of convective heat transfer in unsteady laminar flow over a square cylinder in a channel. *Heat Transfer Engineering*, 26, 21-29.

[14] Bhattacharyya, S. and Mahapatra S. (2005). Vortex shedding around a heated square cylinder under the influence of buoyancy. *Heat and Mass Transfer*, 41, 824-833.

[15] Chatterjee, D. and Mondal B. (2011). Effect of thermal buoyancy on vortex shedding behind a square cylinder in cross-flow at low Reynolds numbers. *International Journal of Heat and Mass Transfer*, 54, 5262-5274.

[16] Sharma, A. and Eswaran V. (2004b). Effect of aiding and opposing buoyancy on the heat and fluid flow across a square cylinder at Re = 100. *Numerical Heat Transfer, Part A: Applications*, 45, 601-624.

[17] Sharma, N., A. Dhiman K. and Kumar S. (2012). Mixed convection flow and heat transfer across a square cylinder under the influence of aiding buoyancy at low Reynolds numbers. *International Journal of Heat and Mass Transfer*, 55, 2601-2614.

[18] Singh, S. K., Panigrahi P. K. and Muralidhar K. (2007). Effect of buoyancy on the wakes of circular and square cylinders: a schlieren-interferometric study. *Experiments in Fluids*, 43, 101-123.

[19] Dhiman, A. K., Chhabra R. P. and Eswaran V. (2008). Steady mixed convection across a confined square cylinder. *International Communications in Heat and Mass Transfer*, 35, 47-55.

[20] Sahu, A. K., Chhabra R. P. and Eswaran V. (2009). Effects of Reynolds and Prandtl numbers on heat transfer from a square cylinder in the unsteady flow regime. *International Journal of Heat and Mass Transfer*, 52, 839-850.

[21] Chatterjee, D. and Biswas G. (2011). The effects of Reynolds and Prandtl numbers on flow and heat transfer across tandem square cylinders in the steady flow regime. *Numerical Heat Transfer, Part A: Applications*, 59, 421-437.

[22] Chatterjee, D. and Amiroudine S. (2010). Two-dimensional mixed convection heat transfer from confined tandem square cylinders in crossflow at low Reynolds numbers. *International Communications in Heat and Mass Transfer*, 37, 7-16.

[23] Waheed, M.A. (2009). "Mixed convective heat transfer in rectangular enclosures driven by a continuously moving horizontal plate". *International Journal of Heat and Mass Transfer*, 52, pp. 5055–5063.

[24] Sangotayo, E. , Adedeji, K. and Ogidiga, J. (2023) Heat Characteristics and Viscous Flow in a Moving Isothermal Cylindrical Duct with Nanoparticles. *Journal of Applied Mathematics and Physics*, 11, 2361-2372. https://doi.org/10.4236/jamp.2023.118151.

[25] Waheed M. A. and Sangotayo, E. O (2013): Numerical Analysis of Dynamic Viscosity Effect Associated with a Continuously Moving Heated Horizontal Plate. *Innovative System Design Engineering Journal*, 4(9) 52-60.

Contribution of Individual Authors to the Creation of a Scientific Article (Ghostwriting Policy)

The authors equally contributed to the present research, at all stages from the formulation of the problem to the final findings and solution.

Sources of Funding for Research Presented in a Scientific Article or Scientific Article Itself

No funding was received for conducting this study.

Conflict of Interest

The authors have no conflicts of interest to declare.